Mutational Analysis of the Base-Flipping Mechanism of Uracil DNA Glycosylase†

Yu Lin Jiang and James T. Stivers*

Department of Pharmacology and Molecular Sciences, The Johns Hopkins University School of Medicine, 725 North Wolfe Street, Baltimore, Maryland 21205-2185

Received May 31, 2002; Revised Manuscript Received July 15, 2002

ABSTRACT: The DNA repair enzyme uracil DNA glycosylase (UDG) locates unwanted uracil bases in genomic DNA using a remarkable base-flipping mechanism in which the entire deoxyuridine nucleotide is rotated from the DNA base stack into the enzyme active site. Enzymatic base flipping has been described as a three-step process involving phosphodiester backbone *pinching*, base extrusion through active *pushing and plugging* by a leucine side chain that inserts in the DNA minor groove, and, finally, *pulling* by hydrogen-bonding groups that interact with the extrahelical base. Here we employ mutagenesis in combination with transient kinetic approaches to assess the functional roles of six conserved enzymatic groups of UDG that have been implicated in the "pinch, push, plug, and pull" base-flipping mechanism. Our results show that these mutant enzymes are capable of flipping the uracil base from the duplex, but that many of these mutations prevent a subsequent induced fit conformational step in which catalytic groups of UDG dock with the flipped-out base. These studies support our previous model for base flipping in which a conformational gating step closely follows base extrusion from the DNA duplex [Stivers, J. T., et al. (1999) *Biochemistry 38*, 952−963]. A model that accounts for the temporal and functional roles of these side chain interactions along the reaction pathway for base flipping is presented.

Enzymes that alter the covalent structure of DNA bases must solve the general problem of gaining access to sites that are normally buried in the duplex structure of the DNA. Nearly 10 years ago the crystal structure of cytosine 5-methyltransferase bound to its DNA substrate revealed that this enzyme solved the problem by a novel base-flipping mechanism involving rotation of the entire cytidine nucleotide from the DNA and into the active site where the 5-position of the cytosine base was positioned for methylation (*1*). Subsequently, it has become clear that base flipping is common in nature, and that many enzymes use similar approaches to act on DNA bases. In particular, base flipping appears to be absolutely required for damaged base recognition and glycosidic bond cleavage by DNA repair glycosylases (*2*−*5*).

Uracil DNA glycosylase (UDG)[1] has taken a paradigm role in the pursuit to better understand the process of base flipping by DNA glycosylases. A crystal structure of human UDG bound to uracil-containing DNA has been reported (*6*), and this structure suggests several structural requirements that may be required for flipping bases (Figure 1A). First, the DNA in this structure is sharply bent by about 45°. If such bending also occurs when UDG first encounters DNA at a nonspecific site, then this distortion may serve to destabilize the duplex and promote uracil flipping when the damaged site is located in correct register with the active site pocket. Bending may be induced by the interaction of two serine side chains with the phosphodiester groups on the 3′ and 5′ sides of the deoxyuridine residue (Ser88 and Ser189), leading to compression of the P−P distance ("serine pinching"). Although induced DNA strain is an attractive mechanism for initiation of the base-flipping process, no direct evidence for this mechanism yet exists. The structure also shows that a completely conserved leucine residue (Leu191) is found protruding into the DNA minor groove opposite the expelled uracil, suggesting that this group acts as a mechanical wedge to "push" the uracil from the duplex (*2*), and additionally as a "plug" to increase its lifetime in the active site (*7*). Recent biochemical studies have provided support for both roles (*7*, *8*). Finally, the uracil base is stabilized in the extrahelical state by a finely tuned hydrogen-bonding network that completely satisfies all of the hydrogen bond donor and acceptor groups of the base (Figure 1A). These hydrogen-bonding interactions have been ascribed a "pulling" function in stabilizing the flipped base (His187 and Asn123) (*9*). Collectively, this constellation of interactions has been termed the "pinch, push, plug, and pull" mechanism for base flipping (*7*, *9*).

Transient kinetic studies and spectroscopic measurements have built upon these structural insights to illuminate the pathway for attaining the final extrahelical state (Figure 1B). One useful approach to isolate the base-flipping step was to arrest the chemical step of the reaction using a deoxyuridine analogue containing an electron-withdrawing 2′-fluorine substituent (2′-FU) (*10*). The kinetics of the base-flipping step could then be monitored in real time using stopped-flow fluorescence, taking advantage of fluorescence intensity changes of a 2-aminopurine fluorescent reporter group that

† Supported by NIH Grant RO1GM56834 (to J.T.S.).

* To whom correspondence should be addressed: Phone: (410) 502-2758. Fax: (410) 955-3023. E-mail: jstivers@jhmi.edu.

[1] Abbreviations: wtUDG, wild-type uracil DNA glycosylase; 2′-FU, 2′-fluoro-2′-deoxyuridine; 2-AP, 2-aminopurine; k_{max}^{trp}, the maximal rate constant in eq 6 for the tryptophan fluorescence change of UDG; k_{max}^{2-AP}, the maximal rate constant in eq 6 for the 2-AP fluorescence change of the DNA.

10.1021/bi026226r CCC: $22.00
Published on Web 08/23/2002

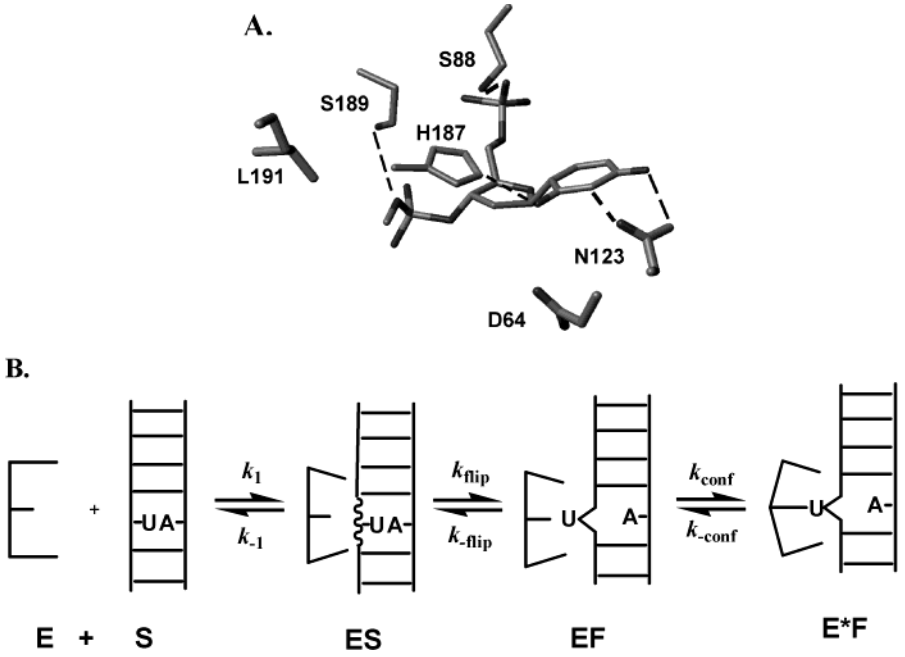

FIGURE 1: (A) Arrangement of the active site groups of UDG that interact with the extrahelical uracil (*6*). The Ser88 and Ser189 phosphodiester pinching residues, the Leu191 pushing and plugging side chain, and the Asn123 and His187 pulling groups are shown. The catalytic group, Asp64, that is important in transition-state stabilization but not base flipping is also shown (*24*). (B) Three-step mechanism for uracil base flipping involving nonspecific DNA binding and dissociation ($k_1 = 220\ \mu M^{-1}\ s^{-1}$, $k_{-1} = 600\ s^{-1}$), reversible uracil flipping into an extrahelical state ($k_{flip} = 700\ s^{-1}$, $k_{-flip} = 180\ s^{-1}$), and conformational docking of UDG around the flipped-out base (k_{conf}, $= 350\ s^{-1}$, $k_{-conf} = 100\ s^{-1}$). The microscopic rate constants were obtained from global kinetic simulations of the stopped-flow kinetic traces (see the Supporting Information and Table 3).

was strategically positioned adjacent to the flipped uracil (*11*). This work revealed that UDG follows a minimal two-step mechanism for base flipping in which a weak nonspecific encounter complex is formed before the uracil is rapidly extruded to form the extrahelical state. Raman spectroscopy measurements indicated that the structure of the nonspecific complex was perturbed, with a significant decrease in the intensities of the DNA base Raman bands, indicating a net increase in base stacking (*12*). A similar hypochromic shift was observed in the specific complex with 2′-FU DNA, suggesting that the nonspecific and specific complexes share common structural features.

Kinetic studies also revealed that uracil flipping is followed closely by a conformational change in UDG that could be monitored by following a decrease in the UDG tryptophan fluorescence, and that this induced fit change only occurs for DNA that contains uracil (Figure 1B) (*10*). This step likely involves the closing of the UDG active site around the flipped uracil, because the free enzyme is found in an open state that differs appreciably from its conformation in the specific complex (*2*, *6*, *13*, *14*). This conformational change likely plays a significant role in the high specificity of UDG for cleavage of the uracil base, because closing of the active site is a prerequisite for formation of the specific hydrogen bonds that are essential for leaving group activation (*15*−*18*). These mechanistic insights initially derived from transient kinetic studies using 2′-FU substrate analogue DNA have been recently confirmed using natural deoxyuridine-containing DNA (*19*).

Here we extend our studies of enzymatic base flipping by selectively deleting the enzymatic side chains that are involved in the pinch, push, plug, and pull mechanism (Figure 1A). We interrogate the resultant effects on the multistep process of base flipping using both thermodynamic and transient kinetic measurements. We have found that a single deletion of either serine pinching side chain does not prevent UDG from flipping the uracil base or undergoing the conformational clamping step. However, removal of *both* serine pinching groups or, alternatively, deletion of the Leu191 or Asn123 side chains prevents the UDG active site from clamping around the extrahelical base. These mutations perturb the base-flipping process at discrete points along the reaction pathway, thereby allowing the temporal mapping of these interactions. In the following paper in this issue (*23*), we extend our recent "substrate rescue" approach to demonstrate how these base-flipping phenotypes can be partially or fully rescued by preorganizing the uracil in an extrahelical conformation using an unnatural pyrene (Y) nucleotide wedge (i.e., a U/Y base pair) (*7*).

EXPERIMENTAL PROCEDURES

Nucleoside Phosphoramidite and Oligonucleotide Synthesis. The nucleoside phosphoramidites were purchased from Applied Biosystems or Glen Research (Sterling, VA), except for the 2′-β-fluoro-2′-deoxyuridine phosphoramidite, which was synthesized as described (*10*). The oligonucleotides were synthesized using standard phosphoramidite chemistry with an Applied Biosystems 390 synthesizer. After synthesis and deprotection, the oligonucleotides were purified by anion exchange HPLC and desalted by C-18 reversed-phase HPLC (Phenomenex Aqua column). The size, purity, and nucleotide composition of the DNA were assessed by analytical reversed-phase HPLC, MALDI mass spectrometry, and denaturing polyacrylamide gel electrophoresis. The DNA strands were hybridized as previously described to form the duplexes used in the binding and kinetic studies as shown in Table 1. In these sequences, U^F = 2′-β-fluoro-2′-deoxyuridine nucleotide. The concentrations of the oligo-

Table 1: DNA Sequences[a]

DNA	Sequence
AU^F/A	GCGCA**U**^{F}AGTCG
	CGCGT**A** TCAGC
PU^F/A	GCGCP**U**^{F}AGTCG
	CGCGT**A** TCAGC

[a] Thermal melting experiments were performed in TMN buffer using 3 μM concentrations of each duplex (see the Experimental Procedures). The melting temperatures for AU^F/A and PU^F/A were 48.8 and 45.8 °C, respectively.

nucleotides were determined by UV absorption measurements at 260 nm, using the pairwise extinction coefficients for the constituent nucleotides.

Purification of UDG and Mutants. As previously described, the recombinant UDG from *E. coli* strain B was purified to >99% homogeneity using a T7 polymerase-based overexpression system (*13*, *20*). The concentration of the enzyme was determined using an extinction coefficient of 38.5 mM^{-1} cm^{-1}. All of the mutations in this work were generated using the Quick-Change double-stranded mutagenesis kit from Stratagene (La Jolla, CA), and the mutations were confirmed by sequencing both strands of the DNA. The 6X-His-tagged mutant proteins were purified using nickel chelate chromatography as previously described (*14*, *20*). The His-tag was removed by cleavage using biotinylated thrombin followed by purification using strepavidin beads and nickel chelate chromatography. The purity of the mutant enzymes was greater than 95% as judged by SDS−polyacrylamide gel electrophoresis with visualization by Coomassie Blue staining.

DNA Binding and Competitive Inhibition Studies. The dissociation constants (K_D) for binding of the various enzymes to the DNA molecules listed in Table 1 were determined using two orthogonal methods. All measurements were performed in TMN buffer, 10 mM Tris−HCl (pH 8.0), 2.5 mM $MgCl_2$, 25 mM NaCl, at 25 °C. In the first method, direct binding measurements were made by following the increase in 2-AP fluorescence upon titrating fixed concentrations of the 2-AP-containing DNA (Figure 2) with increasing amounts of UDG. Excitation was at 320 nm, and emission spectra from 330 to 450 nm were collected using a Spex Fluoromax 3 fluorimeter. The 2-AP fluorescence intensity (F) at 370 nm was plotted against $[UDG]_{tot}$ to obtain the K_D from eqs 1 and 2.

$$F = F_o - \{(F_o - F_f)[DNA]_{tot}/2\} \times \{b - (b^2 - 4[UDG]_{tot}[DNA]_{tot})^{1/2}\} \quad (1)$$

$$b = K_D + [UDG]_{tot} + [DNA]_{tot} \quad (2)$$

Tryptophan Fluorescence Measurements. Dissociation constants were also determined by following the tryptophan fluorescence decrease in UDG as DNA binds (*10*). For these experiments, excitation was at 290 nm and emission scans were performed over the range 305−450 nm. Corrections for dilution and inner filter effects were made using the equation $F_{corr}(335\ nm) = F_{obsd} \times 10^{A^{290}/2}$, where A^{290} is the absorption of the DNA ligand at the excitation wavelength. F_{corr} was then plotted against $[DNA]_{tot}$ to obtain the K_D using eq 1. For the binding measurements using tryptophan fluorescence, the nonfluroescent AU^F/A duplex was used (Table 1).

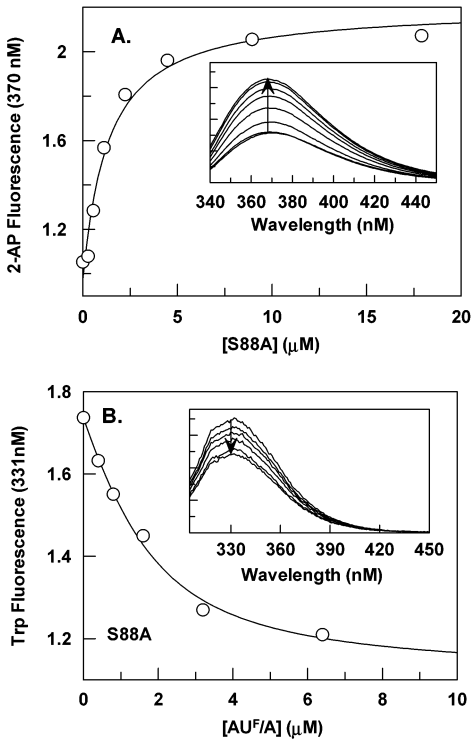

FIGURE 2: Specific DNA Binding of S88A UDG. (A) PU^F/A DNA (1500 nM) was titrated with increasing amounts of S88A, and the 2-AP fluorescence increase at 370 nm is plotted as a function of [S88A]. The curve is the best fit to eq 1. (B) S88A (1500 nM) was titrated with increasing amounts of AU^F/A DNA, and the tryptophan fluorescence decrease at 335 nm is plotted as a function of [AU^F/A]. The K_D values are reported in Table 2.

Fluorescence Measurements of Association and Dissociation Rate Constants. The observed rate constants for association of 2-AP-labeled DNA molecules with the various enzymes were obtained using an Applied Photophysics 720 stopped-flow fluorescence instrument (Surrey, U.K.) using pseudo-first-order conditions in which the concentration of the enzyme was always more than 4-fold greater than the concentration of the labeled DNA. In these experiments a syringe containing a solution of enzyme was rapidly mixed with a solution of labeled DNA delivered from a second syringe. The fluorescence change as a function of time was recorded using a 360 nm cutoff filter with excitation at 320 nm. For stopped-flow measurements in which changes in UDG tryptophan fluorescence were followed, excitation was at 290 nm and emission was monitored at wavelengths greater than 320 nm. In all experiments in which tryptophan fluorescence was followed, the AU/A nonfluorescent substrate was used. The kinetic traces were fitted to a first-order rate expression (eq 3)

$$F_t = \Delta F \exp(1 - k_{obsd}t) + F_o \quad (3)$$

to obtain the observed rate constants (k_{obsd}) at each concentration of enzyme or DNA. With some mutant enzymes, the k_{obsd} values showed a linear dependence on [E], indicating a

simple one-step binding mechanism (eq 4) or, alternatively, a multistep mechanism in which bimolecular association is fully rate-limiting at all achievable concentrations of enzyme. Accordingly, the association rate was obtained from the slope of a plot of k_{obsd} against [E], and k_{on} and k_{off} were obtained from the slope and intercept of the linear regression best-fit line to the data (eq 5). With other mutant enzymes plots of k_{obsd} against [AU^F/A] showed curvature, indicating a more complex multistep binding mechanism. In these cases the data were fitted as described below for wtUDG.

$$E + U \underset{k_{off}}{\overset{k_{on}}{\rightleftharpoons}} E{\cdot}DNA \quad (4)$$

$$k_{obsd} = k_{on}[DNA] + k_{off} \quad (5)$$

For wild-type UDG, curvature in the plot of k_{obsd} against [E] or [DNA] was observed, indicating a change in rate-limiting step from bimolecular association to unimolecular isomerization of the DNA or enzyme (*10*, *21*). Thus, the plot of k_{obsd} against [E] was fitted to eq 6, which is the general analytical solution for the hyperbolic concentration dependence of a minimal two-step base-flipping mechanism (eq 7).

$$k_{obsd} = \frac{K'[E]k_{max} + k_{off}}{(K'[E] + 1)} \quad (6)$$

$$E + S \underset{k_{-1}}{\overset{k_1}{\rightleftharpoons}} ES \underset{k_{-2}}{\overset{k_2}{\rightleftharpoons}} E^*F \quad (7)$$

[As noted previously (*10*), there are no observed kinetic lags in the binding of UDG to DNA because of the rapid rate constants k_{-1}, k_2, and k_{-2} in eq 7. Thus, k_{obsd} is always a single exponential with a hyperbolic dependence on DNA or enzyme concentration.] In eq 6, the initial slope of the hyperbolic concentration dependence provides the apparent second-order rate constant for association of the enzyme with the DNA [$k_{on} = K'k_{max}$, where $K' = k_1/(k_{-1} + k_{max})$], the asymptotic value provides the observed rate constant for reversible base flipping ($k_{max} = k_2 + k_{-2}$), and the *y* intercept provides the dissociation rate constant [$k_{off} = k_{-1}k_{-2}/(k_{-1} + k_{max})$]. In this minimal two-step mechanism, the base-flipping step ($k_{max} = k_2 + k_{-2}$) is a composite of the base extrusion and UDG isomerization steps shown in Figure 1B (*10*). Depending on whether 2-AP or tryptophan fluorescence is followed, k_{max} is designated as k_{max}^{2-AP} or k_{max}^{trp}, respectively. An equation of form identical to that of eq 6 can result if more than two steps are involved, but the microscopic rate constants that comprise the apparent constants K', k_{max}, and k_{off} will differ. A three-step mechanism, such as that shown in Figure 1B, is best analyzed by computer simulation of the kinetic data (see below). Regardless of whether eq 5, eq 6, or a more complex three-step binding mechanism is used to analyze the data, $k_{off}/k_{on} = K_D$, the overall dissociation constant for the interaction. The apparent rate constants obtained from these analytical expressions are more accurate than the microscopic rate constants obtained from computer simulations, and provide informative parameters for comparison of the kinetic properties of the wild-type and mutant enzymes.

To augment the approach-to-equilibrium kinetic measurements, the dissociation rate constant (k_{off}) of U/A from the various enzymes was also measured using irreversible conditions. When 2-AP fluorescence was followed, these experiments were carried out by rapidly mixing a preformed enzyme−DNA complex with a large excess of nonfluorescent single-stranded trapping DNA. The sequence of the trap DNA was the same as that of the AU^FA strand of the duplex (Table 1). The time-dependent decrease in 2-AP fluorescence was then followed using the stopped-flow fluorescence instrument. When tryptophan fluorescence was followed, the free enzyme was trapped using a high concentration of nonspecific DNA (50 μM). In all cases, the kinetic traces were fitted to a single-exponential decay (eq 8). Further experimental details may be found in the figure captions.

$$F_t = \Delta F \exp(-kt) + F_o \quad (8)$$

Computer Simulations. The values for k_{on}, k_{off}, k_{max}, and K_D were used as starting values to constrain simulations in which the microscopic rate constants for a more complex three-step mechanism for base flipping were determined (Figure 1B). The simulations were performed by globally fitting the kinetic traces to a single set of six microscopic rate constants as defined in the three-step mechanism depicted in Figure 1B (k_{-1}, k_1, k_{flip}, k_{-flip}, k_{conf}, k_{-conf}) using the program Dynafit (*22*). The requirement for a three-step mechanism in which the conformational clamping step of UDG lags behind the initial extrusion of the uracil was suggested by the observation that the k_{max}^{trp} value obtained from following the tryptophan fluorescence of UDG was about 40% less than the k_{max}^{2-AP} value obtained from following the 2-AP fluorescence of the DNA (see the Results and Discussion).

RESULTS AND DISCUSSION

Definitions. To allow facile comparison of the mutational effects with the pyrene rescue effects reported in the following paper (*23*), we have defined the mutational effect as the kinetic (or binding) parameter for the wild-type enzyme divided by that for the mutant enzyme. Thus, effects greater than unity always indicate a fold *damaging* effect on a rate constant (i.e., a slower on-rate or faster off-rate) or a *weakening* of binding affinity as a result of the mutation. To maintain consistency and simplicity in the description of the effects, we report the mutational effects on the off-rate and K_D values as (wild-type value)$^{-1}$/(mutant value)$^{-1}$ such that ratios greater than unity still reflect the fold damaging effect of the mutation.[2]

Mutational Effects on DNA Binding. Eight different UDG mutations are investigated in this study (Figure 1A): three serine mutations that remove the hydroxyl groups that are proposed to *pinch* the phosphodiester backbone (S88A, S189A, S88A:S189A), two leucine mutations that lack the bulky side chain that *pushes* into the minor groove (L191A, L191G), asparagine and histidine mutations (N123G, H187G) that remove hydrogen-bonding groups that *pull* on the uracil by bonding to O2, O4, and N3, and an aspartate mutation that removes the water activating group (D64N). These mutations probe the four components of the pinch, push,

[2] The effects of these mutations on the steady-state kinetic parameters of UDG have also been measured and will be reported elsewhere (Jiang and Stivers, manuscript in preparation).

Table 2: Equilibrium and Kinetic Constants for Binding of Mutant UDG Enzymes to U^F/A DNA Analogues[a]

enzyme	substrate	k_{on} (μM^{-1} s^{-1})	k_{off} (s^{-1})	k_{max} (s^{-1})	K' (μM^{-1})	k_{off}/k_{on} (μM)	K_D (μM)
wtUDG	PU^F/A	160 ± 6	21 ± 3	650 ± 43	0.40 ± 0.08	0.13 ± 0.02	0.13 ± 0.03
	AU^F/A	120 ± 11	22 ± 5	400 ± 10	0.3 ± 0.03	0.18 ± 0.04	0.11 ± 0.02
S88A	PU^F/A	47 ± 15	80 ± 15	≥650[b]	0.032 ± 0.002	1.7 ± 0.5	1.2 ± 0.3
	AU^F/A	34 ± 14	88 ± 6	680 ± 110	0.05 ± 0.016	2.6 ± 1.2	1.1 ± 0.2
S189A	PU^F/A	46 ± 5	23 ± 1	650 ± 170	0.09 ± 0.03	0.47 ± 0.05	0.62 ± 0.06
	AU^F/A	13 ± 5	8 ± 3	210 ± 40	0.06 ± 0.02	0.6 ± 0.2	0.33 ± 0.03
S88A:S189A	PU^F/A	14 ± 3	205 ± 30			14 ± 4	8.4 ± 1.4
L191A	PU^F/A	20 ± 6	56 ± 12			2.8 ± 1.0	0.95 ± 0.05
L191G	PU^F/A	9.9 ± 1.9	93 ± 20			9.4 ± 2.7	5.1 ± 1.5
N123G	PU/A						2.1 ± 0.4[c]
H187G	PU^F/A	34 ± 5	4.6 ± 0.5			0.14 ± 0.03	0.28 ± 0.04
D64N	PU^F/A	216 ± 9	8.9 ± 0.5			0.041 ± 0.003	0.020 ± 0.002

[a] Some of the equilibrium binding parameters for wtUDG have been previously published (*7*). The parameters k_{on}, k_{off}, k_{max}, and K' are defined in eqs 6 and 7. The k_{max} values for AU^F/A were obtained from the rates of tryptophan fluorescence changes in UDG (k_{max}^{trp}). The k_{max} values for PU^F/A were obtained from the rates of 2-AP fluorescence changes of the DNA (k_{max}^{2-AP}). The parameters for PU^F/A and AU^F/A were determined in stopped-flow experiments by following the 2-AP fluorescence of the DNA or the tryptophan fluorescence of UDG, respectively. [b] Only a lower limit value was obtained with the S88A mutant. [c] This is the K_m value of N123G for the corresponding substrate. Binding measurements with PU^F/A were complicated by apparent sigmoidicity, which was not observed in the kinetic measurements (data not shown).

Table 3: Microscopic Rate Constants for a Three-Step Base-Flipping Mechanism by wtUDG Determined from Kinetic Simulations[a]

k_1 (μM^{-1} s^{-1})	k_{-1} (s^{-1})	k_{flip} (s^{-1})	k_{-flip} (s^{-1})	k_{conf} (s^{-1})	k_{-conf} (s^{-1})	$K_{flip}K_{conf}$[b]
220 ± 50	600 ± 100	700 ± 200	180 ± 50	350 ± 50	100 ± 10	14 ± 4

[a] The rate constants were obtained from global simulations of the transient kinetic data shown in Figure 4A,B,D,E using the program Dynafit (*22*) and correspond to the steps in Figure 1B. The simulated fits to the data and the Dynafit script files are provided in the Supporting Information. A unique fit to the data required an estimate for the equilibrium constant for the first nonspecific binding step. This estimate ($K_D^{ns} = 3.6 \pm 0.5$ μM) was obtained for an 11-mer duplex using competition binding measurements as previously described (*7*). The off-rate of nonspecific DNA (k_{-1} = 400−750 s^{-1}) has been previously estimated (*10*). These estimates for K_D^{ns} and k_{-1} are in good agreement with fluorescence binding measurements using a nonspecific pyrene-containing 11-mer duplex ($K_D^{ns} = 2.7 \pm 0.3$ μM, $k_{-1} = 440 \pm 40$ s^{-1}). The data were also constrained by the overall dissociation constant $K_D = (K_1K_{flip}K_{conf})^{-1} = 0.15 \pm 0.04$ μM (average value). The estimated errors in the microscopic constants are based on systematic sweeping of the individual rate constants over a 4-fold range, and then comparing visual fits to all the rate and equilibrium data. The final optimized fits to all of the kinetic data were obtained by constrained nonlinear regression fitting using the same set of six microscopic rate constants (a ±10% deviation in the rate constants was allowed during fitting). The reported values are average values obtained from fitting all of the four data sets. [b] $K_{flip}K_{conf}$ is the overall equilibrium constant for base flipping on the enzyme ([E*F]/[ES]). This product of equilibrium constants is comparable to the previously reported net equilibrium constant for base flipping based on a two-step mechanism ($K_{flip} = 19 \pm 8$ for a U/A base pair) (*10*).

plug, and pull mechanism for base flipping (*2*, *7*). The characterization of D64N mutation serves as a useful control for the specificity of the substrate rescue effects that are reported in the following paper (*23*). This aspartate group has previously been shown to have no detrimental effect on DNA binding or base flipping, and mainly serves to stabilize the ionic transition state and intermediate for glycosidic bond cleavage by an electrostatic mechanism (*24*). Thus, the preorganized substrate with the pyrene wedge would not be expected to rescue the ~3000-fold damaging effect of removing Asp64 (*7*).

Binding of Wild-Type and Mutant Enzymes to U^F/A Analogues. To begin the mutational analysis, we performed DNA binding measurements using the nonreactive substrate analogue constructs PU^F/A and AU^F/A employing the 2-AP and tryptophan fluorescence assays. The 2-AP fluorescence is very sensitive to base-stacking interactions and reports on the expulsion of the uracil from the duplex, while the tryptophan fluorescence detects the postflipping conformational change in UDG. We have employed 11-mer duplex substrates in this study because of concerns that longer DNA sequences, such as the 19-mer used in a previous study (*10*), might lead to a significant amount of nonspecific DNA binding for the base-flipping mutants. Accordingly, we have truncated the DNA to a minimal length that maintains essentially full catalytic activity as observed previously for longer DNA molecules (*7*, *25*). Several crystal structures of human UDG productively bound to DNA duplexes of this size have been solved, indicating that these 11-mers capture all of the interactions required for base flipping and catalysis (*2*, *6*, *14*). The K_D values for wtUDG are reported in Table 2 for comparison with those of the mutants.

Representative binding data for the S88A "pinching" mutant using the 2-AP and tryptophan fluorescence assays are shown in parts A and B, respectively, of Figure 2. The K_D values obtained from these data are 1.2 ± 0.3 and 1.1 ± 0.2 μM (Table 2), which indicates that removal of the hydroxyl group of Ser88 weakens binding by 9-fold as compared to that of wtUDG (Table 4). Analogous measurements were performed for the other mutations, and the K_D values and mutational effects are reported in Tables 2 and 4, respectively. In general, the binding defects arising from removal of the Ser88, Ser189, and L191 side chains are in the range 5−40-fold, with the largest effect being observed for the L191G "pushing" mutation. The double mutation, S88A:S189A, shows a 65-fold detrimental effect on binding, which is only modestly greater than the 44-fold damaging effect expected from multiplying the individual effects of each single mutation.

We observed a large difference between the mutational effects of removing the two side chains that hydrogen bond with the flipped-out uracil (Asn123 and His187), indicating distinct roles for these two "pulling" groups (Tables 2 and 4). The N123G mutation binds 16-fold more weakly than

Table 4: Mutational Effects on DNA Binding, Association, and Dissociation[a]

		fold mutational effect			
enzyme	DNA	$1/K_D$	k_{on}	$1/k_{off}$	k_{max}
S88A	PU^F/A	9.2	3.4	3.8	*b*
	AU^F/A	10	3.5	4	0.59
S189A	PU^F/A	4.8	3.5	1.1	1
	AU^F/A	3	9.2	0.36	1.9
S88A:S189A	PU^F/A	65	11	9.8	
L191A	PU^F/A	7.3	8	2.7	
L191G	PU^F/A	39	16	4.4	
N123G	PU^F/A	16			
H187G	PU^F/A	2.1	4.7	0.22	
D64N	PU^F/A	0.15	0.74	0.42	

[a] Mutational effects are defined as wild-type value/mutant value. Therefore, effects greater than unity indicate a damaging effect of the mutation (i.e., a decrease in the on-rate or an increase in the off-rate or K_D). All values are derived from measurements using the PU^F/A analogue except for the effects on the S88A and S189A mutants, which were obtained with both the AU^F/A and PU^F/A analogues as indicated. The definitions of the parameters may be found in eqs 4−7. The average error for all the mutational effects is ±14%; the largest errors are less than ±30%. [b] Only a lower limit value for k_{max}^{2-AP} of ~650 s^{-1} was obtained for S88A.

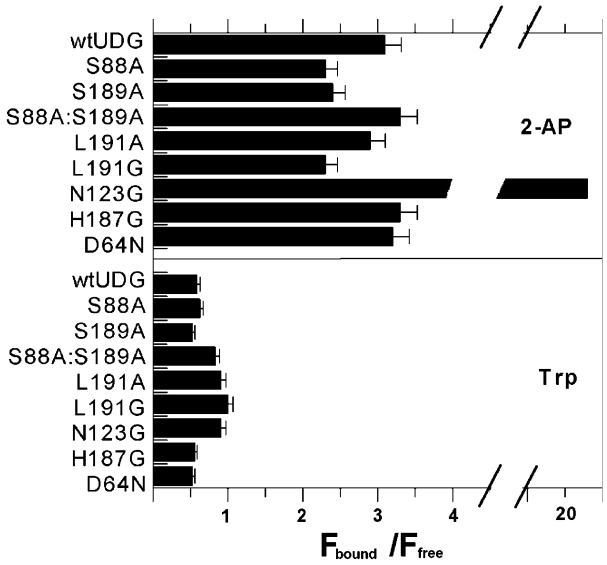

FIGURE 3: Maximal changes in DNA 2-AP fluorescence and UDG tryptophan fluorescence. The changes are reported as the ratio F_{bound}/F_{free}, where F_{bound} is the fluorescence of the PU^F/A DNA or enzyme at saturation and F_{free} is the fluorescence of the free DNA or enzyme.

wtUDG as determined from its $K_m = 2.1 \pm 0.4$ μM, which was measured using the 2-AP steady-state kinetic assay (*11*). In contrast, the H187G mutation has a small 2-fold detrimental effect on DNA binding, even though this mutation has a ~4000-fold damaging effect on the activation barrier (*20*, *26*). Thus, Asn123 interacts strongly with the O4 and H3 atoms of the uracil in the ground state, while the strong hydrogen bond between uracil O2 and H^ϵ of His187 develops later during the transition state for glycosidic bond cleavage (*17*, *18*). As we have previously observed, the D64N mutation actually enhances binding by about 8-fold, which we have attributed to ablation of an unfavorable electrostatic interaction between Asp64 and the anionic phosphodiester backbone of the DNA (*7*).

Nature of the Extrahelical State for Each Mutant. Several of the mutant enzymes that showed substantial increases in 2-AP fluorescence did not show any decrease in tryptophan fluorescence upon binding of AU^F/A, indicating that these enzymes were defective in the postflipping conformational change in UDG (*10*). Shown in Figure 3 are the maximal 2-AP and tryptophan fluorescence changes for wtUDG and each mutant (F_{bound}/F_{free}). The S88A:S189A, L191A, H187G, and D64N enzymes show almost the same F_{bound}/F_{free} for binding PU^F/A as the wild-type enzyme (F_{bound}/F_{free}(wtUDG) $= 3.1 \pm 0.2$), indicating that for these enzymes the DNA adopts a conformation similar to that found in the wild-type enzyme. The ratio F_{bound}/F_{free} for the S88A, S189A, and L191G mutants is approximately 35% smaller than that for wtUDG, suggesting modest differences in the extrahelical state that is detected by 2-AP fluorescence for these enzymes.

Most of the mutants show tryptophan fluorescence decreases upon DNA binding that are similar to those of wtUDG (F_{bound}/F_{free}(Trp) $= 0.59 \pm 0.05$) (Figure 4). However, neither the Leu191 deletion mutants nor the N123G and serine double mutant shows a significant decrease. These results strongly indicate that removal of these groups severely alters the internal equilibrium for the conformational docking step that is required to lock in the flipped-out uracil (k_{conf}/k_{-conf}, Figure 1B). Given that a significant 2-AP fluorescence increase was detected with these mutants, the absence of a tryptophan fluorescence decrease suggests that the reaction has been arrested at an otherwise sparsely populated intermediate in which the uracil is extrahelical, but the enzyme has not yet enveloped the base. These results support our two previous studies of base flipping where we concluded that uracil expulsion was followed closely by a conformational change in UDG (*10*), and that part of the action of Leu191 *followed* the complete or partial expulsion of the uracil from the base stack (*7*, *8*). Further insights into the roles of Leu191 are suggested from the binding and kinetic studies described below.

The fluorescence studies indicate that the N123G mutation results in a highly unusual binding mode, leading to an increased unstacking of the 2-AP base (Figure 3). Binding of the N123G mutant to PU^F/A gives rise to an anomalous 21-fold increase in 2-AP fluorescence that is 7-fold *larger* than that of wild-type UDG.

Transient Kinetic Studies of Base Flipping by Wild-Type UDG. Although we have already investigated the kinetic process of base flipping by UDG using a 19-mer DNA in which the uracil was located in an A tract sequence (*10*), the significantly different substrates used here required further measurements. This was especially important because of the strong DNA sequence dependence of the UDG activity (*25*, *27*, *28*). The approach we have taken is based on our previous findings that base flipping and the postflipping conformational change in UDG can be followed using the 2-AP fluorescence increase of the DNA, or the tryptophan fluorescence decrease of UDG, respectively (*10*).

Several stopped-flow kinetic traces for approach-to-equilibrium binding of the PU^F/A 11-mer to wtUDG are shown in Figure 4A in which the increase in 2-AP fluorescence is followed. We also measured the off-rate of PU^F/A from wtUDG using irreversible conditions in which the dissociated enzyme was trapped by a large excess of nonfluorescent 11-mer DNA, and the dissociation of this complex was well-fitted as a single-exponential kinetic

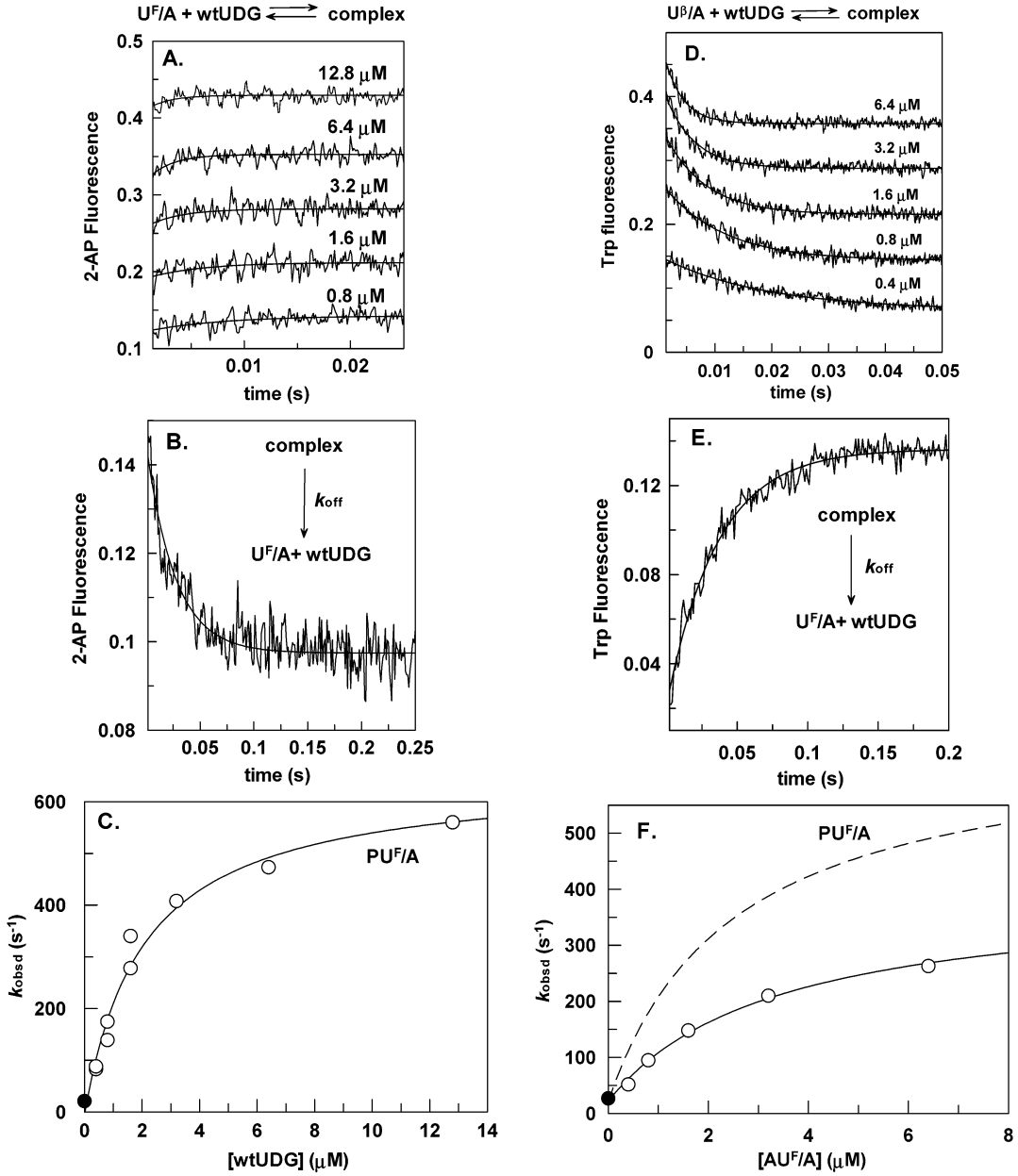

FIGURE 4: Stopped-flow fluorescence kinetic studies of DNA association and dissociation from wtUDG. (A) Approach-to-equilibrium association measurements where 100 nM PU^F/A DNA was mixed with the indicated concentrations of UDG and the 2-AP fluorescence increase was monitored with a 360 nm cutoff filter with excitation at 320 nm. The lines are the fits to a first-order rate equation. (B) Irreversible dissociation of PU^F/A DNA from UDG. A solution of 500 nM PU^F/A DNA and 1 μM UDG was mixed with a 10 μM concentration of an ssAU^F 11-mer nonfluorescent DNA trap to prevent reassociation of the enzyme to PU^F/A. The time-dependent decrease in 2-AP fluorescence was measured. (C) Observed rate constants from (A) (○) and (B) (●) against [wtUDG]. The curve is a best fit to eq 6. (D) Approach-to-equilibrium association measurements where 100 nM UDG was mixed with the indicated concentrations of AU^F/A DNA and the tryptophan fluorescence decrease was monitored with a 320 nm cutoff filter with excitation at 290 nm. The lines are fits to a first-order decay rate equation. (E) Irreversible dissociation of AU^F/A DNA from UDG as monitored by UDG tryptophan fluorescence. A solution of 500 nM AU^F/A DNA and 1 μM UDG was mixed with a 50 μM concentration of a 19-mer nonfluorescent DNA to trap the enzyme as it dissociated (*10*). The time-dependent increase in 2-AP fluorescence was measured. (F) Observed rate constants from (D) (○) and (E) (●) against [AU^F/A]. The curve is a best fit to eq 6. For comparison, the dashed line is the theoretical curve obtained in (C) from the 2-AP measurements. The parameters are reported in Table 2.

process (Figure 4B). A plot of the observed association rate constants against [wtUDG] is hyperbolic (Figure 4C), suggesting at least a two-step binding mechanism. Fitting these data to eq 6 yields $k_{on} = 160 \pm 6$ μM^{-1} s^{-1}, $k_{off} = 21 \pm 3$ s^{-1}, $K' = 0.40 \pm 0.08$ μM^{-1}, and $k_{max} = 650 \pm 43$ s^{-1} (Table 2). The measured off-rate (closed circle, Figure 4C) agrees very well with the *y* intercept obtained from fitting the observed association rate constants to eq 6 (Figure 4C), and the ratio $k_{off}/k_{on} = 0.13 \pm 0.02$ is in excellent agreement with the measured $K_D = 0.13 \pm 0.05$ (Table 2). The single-exponential off-rate of PU^F/A from wtUDG indicates that the multistep process of DNA dissociation has *one* major rate-limiting transition state. Further studies described below indicate that this transition state is for the reverse conformational change shown in Figure 1B (k_{-conf}).

The hyperbolic concentration dependence of k_{obsd} for wtUDG binding to PU^F/A indicates a change in rate-limiting step from concentration-dependent association of the enzyme

with the DNA to concentration-independent isomerization of the enzyme−DNA complex. These results using the PU^F/A 11-mer are similar to those previously reported using a U^F/A 19-mer duplex in which the uracil was located in an A-rich tract (5′-AAPU^{F}AAAAA-3′). With the previous 19-mer, $k_{on} = 320 \pm 50\ \mu M^{-1}\ s^{-1}$, $k_{off} = 28 \pm 2\ s^{-1}$, $K_D = 0.09 \pm 0.02$, and $k_{max} = 1200 \pm 200\ s^{-1}$. The 1.8-fold larger k_{max} value, and the 1.6-fold tighter binding of the 19-mer as compared to the 11-mer, quantitatively accounts for the observation that the 19-mer shows a 1.6-fold larger increase in 2-AP fluorescence upon UDG binding as compared to the 11-mer used here (*10*). These results indicate that the base-flipping rates (k_{flip} and k_{-flip}), and the equilibrium constant for base flipping ($K_{flip} = k_{flip}/k_{-flip}$) may be modestly affected by the sequence context in which the uracil is located. DNA sequence effects on the steady-state k_{cat}/K_m for human (*27*), *E. coli* (*25*), and herpes virus UDG (*28*) have been reported, and the results here suggest that part of the k_{cat}/K_m effects may arise from a DNA sequence dependence of the base-flipping step.

We also followed the forward binding kinetics and the reverse dissociation kinetics by monitoring tryptophan fluorescence of wtUDG (Figure 4D,E). The closing of the UDG clamp upon AU^F/A binding results in a 1.7-fold decrease in tryptophan fluorescence, and the reverse clamp-opening step results in a recovery of tryptophan fluorescence of the same magnitude. The observed rate constants for AU^F/A binding showed a hyperbolic dependence on [AU^F/A] similar to that seen when the 2-AP fluorescence of PU^F/A was monitored (Figure 4F). Although the values $k_{on} = 120 \pm 11\ \mu M^{-1}\ s^{-1}$, $k_{off} = 22 \pm 5\ s^{-1}$, and $K' = 0.3 \pm 0.03\ \mu M^{-1}$ were similar to those measured by following the 2-AP fluorescence, the k_{max} value was found to be 40% smaller ($k_{max} = 400 \pm 10\ s^{-1}$). (For comparison, the best-fit curve from fitting the k_{obsd} values obtained using 2-AP fluorescence is shown as a dashed line in Figure 4F.) An important observation from these data is that the off-rates measured using tryptophan and 2-AP fluorescence are *identical* (Figure 4B,E). This result indicates that the same rate-limiting step is detected in both experiments, and requires that opening of the conformational clamp (k_{-conf} in Figure 1B) is slow compared to the reverse step of base flipping (k_{-flip}) and DNA dissociation (k_{-1}).

A Three-Step Mechanism for Uracil Flipping. The 40% higher k_{max} value that was measured using the 2-AP fluorescence signal strongly indicates that the UDG conformational change slightly lags behind the base-flipping step with these substrates that contain a U/A base pair. Our previous study using a 19-mer DNA with a significantly different sequence surrounding the U^F/A base pair showed smaller rate differences for the 2-AP and tryptophan fluorescence changes (*10*). These differences were hardly beyond the error limits in the measurements [k_{max}(2-AP) = 1200 ± 200 s^{-1}, k_{max}(trp) = 800 ± 200 s^{-1}], but we concluded that base flipping was "followed closely by a conformational change in UDG". Because the binding kinetics and mutational effects reported below clearly reveal that the conformational change lags behind the flipping step, we have used global kinetic simulation of the data to obtain the microscopic rate constants for a three-step mechanism (Figure 1B). The kinetic constants obtained from these simulations are $k_1 = 220 \pm 50$, $k_{-1} = 600 \pm 100\ s^{-1}$, $k_{flip} = 700 \pm 200\ s^{-1}$, $k_{-flip} = 180 \pm 50\ s^{-1}$, $k_{conf} = 350 \pm 50\ s^{-1}$, and $k_{-conf} = 100 \pm 10\ s^{-1}$; $K_{flip}K_{conf} = 14 \pm 4$ (Table 3). The simulated fits to the individual kinetic traces are shown in the Supporting Information.

Kinetic Roles of the Pinch, Push, Plug, and Pull Groups. Analogous stopped-flow fluorescence experiments were performed for each mutant to assess whether each side chain interaction was important for the forward rate of DNA association or, alternatively, served to stabilize the major extrahelical state (E*F, Figure 1B). Representative kinetic experiments for binding of L191A to PU^F/A are shown in Figure 5 in which changes in 2-AP fluorescence were followed. From the linear plot of k_{obsd} against [L191A] in Figure 5C we obtained $k_{on} = 20 \pm 6\ \mu M^{-1}\ s^{-1}$ and $k_{off} = 56 \pm 12\ s^{-1}$. Thus, for L191A, k_{on} is decreased by 8-fold and k_{off} is increased by 3-fold as compared to those of wtUDG, while slightly larger effects of 16-fold and 4.4-fold were measured for the L191G mutant (Tables 2 and 4, data not shown). L191A did not show any evidence of curvature in the plots of k_{obsd} against [enzyme] when the PU^F/A substrate was used, indicating that bimolecular association was slower than any subsequent isomerization events that may be occurring. It should be reemphasized that L191A (as well as L191G and S88A:S189A) does not proceed to the conformational docking step that results in tryptophan fluorescence quenching of wtUDG (Figure 4). Thus, the kinetic results for L191A binding to PU^F/A measure the observed rate for formation of a metastable extrahelical intermediate that most likely resembles the EF complex in Figure 1B.

Since the S88A and S189A serine pinching mutants both showed tryptophan fluorescence decreases upon binding AU^F/A (Figure 3), it was possible to probe the binding kinetics by following 2-AP fluorescence and tryptophan fluorescence. Both of these enzymes bind DNA weakly, and show a lesser increase in 2-AP fluorescence than the wild-type enzyme, which led to very weak signal changes when using the 2-AP assay (Figure 6A). Nevertheless, the results were reproducible on different days, with different batches of enzyme and DNA, and the approach-to-equilibrium kinetic results were in good or excellent agreement with both the thermodynamic measurements and the irreversible off-rate measurements (Table 2). In addition, the tryptophan fluorescence measurements were more robust than the 2-AP measurements (compare parts A and B of Figure 6), and yielded results that were consistent with those obtained using the 2-AP probe. For both the S88A and S189A mutants (Figure 6C,D), the plots of k_{obsd} against enzyme concentration were slightly curved when 2-AP fluorescence was followed, but were distinctly hyperbolic when tryptophan fluorescence was monitored. In addition, the observed rate constants were always faster for the 2-AP fluorescence changes as compared to the tryptophan fluorescence changes. These results are reminiscent of wtUDG where the formation of the extrahelical base was more rapid than the conformational change (Figure 4F), and indicate that the conformational change remains the rate-limiting step for the S88A and S189A mutants. These mutants have 3.5−9-fold slower association rates as compared to wtUDG, showing that these groups play a modest role in facilitating the formation of the extrahelical states (EF and E*F in Figure 1B). However, the rate of the conformational change that is detected by tryptophan fluo-

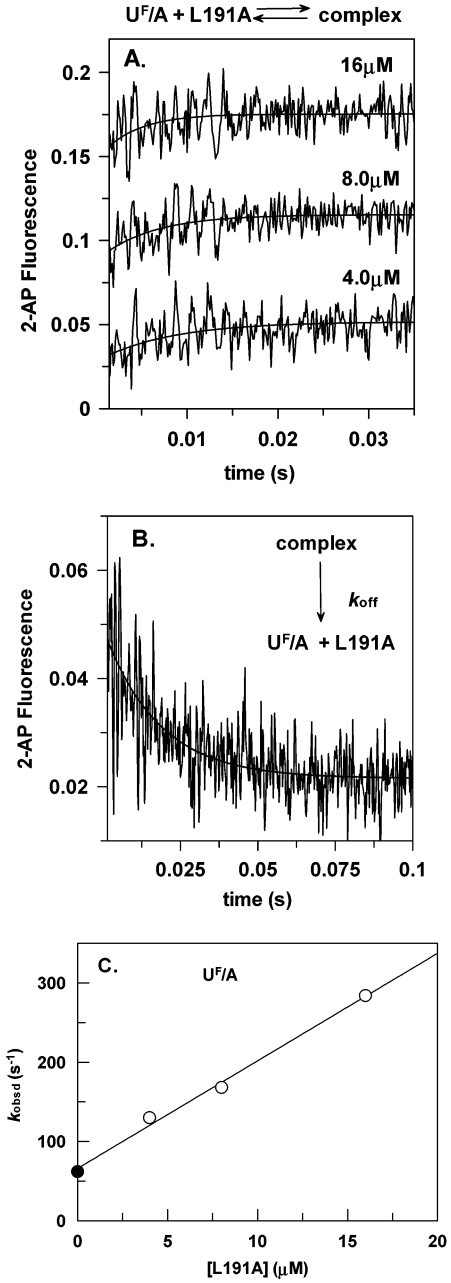

FIGURE 5: Stopped-flow fluorescence kinetic studies of DNA association and dissociation from L191A. (A) Approach-to-equilibrium association measurements where 1 μM PU^F/A DNA was mixed with the indicated concentrations of L191A and the 2-AP fluorescence increase was monitored with a 360 nm cutoff filter with excitation at 320 nm. The lines are the fits to a first-order rate equation. (B) Irreversible dissociation of PU^F/A DNA from L191A. A solution of 500 nM PU^F/A DNA and 1 μM L191A was mixed with a 10 μM concentration of an ssAU^F 11-mer nonfluorescent DNA trap to prevent reassociation of the enzyme to PU^F/A. The time-dependent decrease in 2-AP fluorescence was measured. (C) Observed rate constants from (A) (○) and (B) (●) against [L191A]. The curve is a best fit to eq 5. The parameters are reported in Table 2.

rescence with these mutants is not significantly impaired as compared to the wild-type enzyme (Table 2). Thus, removal of these individual serine side chains does not prevent attainment of the closed conformation as judged by the similar tryptophan fluorescence decreases with wtUDG, nor does it dramatically slow its rate of formation. However, as noted above, removal of *both* side chains in the S88A:S189A double mutant abrogates the conformational change entirely, suggesting cooperative action of these groups in the overall process of attaining this final state that immediately precedes glycosidic bond cleavage. Although these data suggest that the serine mutants follow a three-step mechanism for base flipping like wtUDG, the data do not constrain the modeling sufficiently to allow unambiguous assignment of microscopic rate constants. Therefore, in the analysis of these results below we merely compare the apparent rate constants for the 2-AP and tryptophan fluorescence changes with those of wtUDG.

The N123G and H187G pulling mutations and the D64N control were also investigated using the same kinetic approaches (Tables 2 and 4). Due to the weak DNA binding by N123G, and the total lack of a tryptophan fluorescence change upon DNA binding, we were unable to determine any kinetic constants for this enzyme. Surprisingly, the kinetic measurements with H187G revealed compensating effects on k_{on} and k_{off} (Table 2). That is, the 5-fold decrease in k_{on} is offset by a nearly equal decrease in k_{off}, such that the ratio k_{off}/k_{on} is unchanged from that of the wild-type enzyme (Table 2). Finally, the kinetic studies of D64N indicate that the ~3-fold smaller k_{off}/k_{on} ratio for D64N as compared to wtUDG arises from a 1.3-fold increase in k_{on} and a 2-fold smaller k_{off}. These small effects on DNA binding and base flipping are consistent with the primary function of Asp64 in transition-state stabilization.

CONCLUSIONS

These results allow construction of a temporal pathway for base flipping, and suggest functional roles for the conserved serine, leucine, and asparagine side chains at several steps in the overall process of base flipping (Figure 7). In this model, which is depicted as a free energy reaction coordinate diagram in Figure 7, we assign the temporal formation of these interactions as "early" or "late" in the overall process of forming the final extrahelical state (E*F). The early classification includes all ground states and transition states leading to the metastable state where the uracil is extrahelical and the enzyme is in the open conformation (EF). The late classification includes the transition state and ground state for formation of the closed conformation, which can be monitored by tryptophan fluorescence (E*F). The functional implications suggested here by mutagenesis are further supported by the pyrene substrate rescue studies in the following paper (*23*).

Serine Pinching. Deletion of Ser88 or Ser189, which interact with the 5′ and 3′ phosphodiester groups of the deoxyuridine nucleotide (Figure 1A), results in less than a +1.8 kcal/mol effect on the overall binding equilibrium (Table 4), reflecting perturbations both at early and late steps in the base-flipping pathway (Figure 7). An early and late role for these pinching interactions is suggested by the effect of the S88A:S189A double mutation, which shows an 11-fold decrease in the rate of formation of the metastable intermediate (an early effect), and a strong destabilization of the closed state reflected in the absence of a tryptophan fluorescence change and a large k_{off} (late effects). Serine 88 does not appear to form a strong interaction in the apparent transition state for formation of the closed conformation, because its k_{max}^{trp} is similar to that of wtUDG (Table 2).

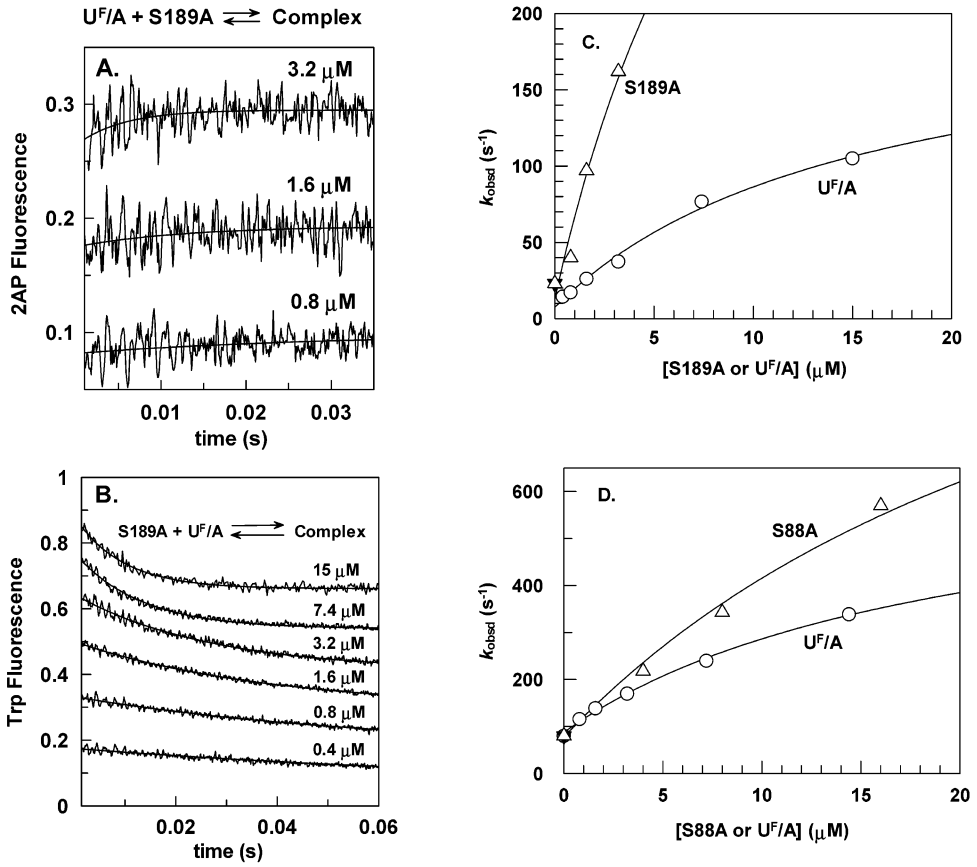

FIGURE 6: Stopped-flow fluorescence kinetic studies of DNA association and dissociation from S189A and S88A. (A) Approach-to-equilibrium association measurements where 200 nM PU^F/A DNA was mixed with the indicated concentrations of S189A and the 2-AP fluorescence increase was monitored with a 360 nm cutoff filter with excitation at 320 nm. The lines are the fits to a first-order rate equation. (B) Approach-to-equilibrium association measurements where 100 nM S189A was mixed with the indicated concentrations of AU^F/A DNA and the tryptophan fluorescence decrease was monitored with a 320 nm cutoff filter with excitation at 290 nm. The lines are fits to a first-order decay rate equation. (C) Observed rate constants from (A) (△) and (B) (○) against [S189A]. The curve is a best fit to eq 6. The kinetic parameters are reported in Table 2. (D) Observed rate constants for S88A binding to PU^F/A (△) and against [AU^F/A] (○). The curve is a best fit to eq 6.

However, a modest interaction of Ser88 in the ground-state E*F complex is indicated by the 4-fold faster off-rate of S88A as compared to wtUDG, suggesting that E*F is destabilized when the Ser88 side chain is removed (Figure 7). In contrast, the 2-fold slower k_{max}^{trp} resulting from the removal of Ser189 is most simply accounted for by a transition-state effect rather than a ground-state effect. This conclusion is supported by the observation that the same ~2-fold damaging effect is seen both in the forward rate of formation of E*F by Ser189A (i.e., k_{max}^{trp}) and in the reverse direction (i.e., k_{off}) (Figure 7). Most importantly, for both S88A and S189A, the off-rates measured using tryptophan fluorescence are equal to or slower than the values measured using the 2-AP probe. Thus, as observed for wtUDG, the reverse conformational change is still the rate-limiting step, and not the reverse flipping or DNA dissociation steps.

Leucine Pushing and Plugging. An early and late role for Leu191 is also suggested. Removal of this side chain destabilizes the closed conformation such that no tryptophan fluorescence changes can be detected, requiring a late role for Leu191 in stabilizing the E*F complex and perhaps in accelerating its formation. Since the major bound DNA form with the Leu191 mutants is the open EF complex, the 8- and 16-fold smaller k_{on} values for these enzymes must reflect the removal of important interactions of this side chain that occur in the early steps of the base-flipping reaction. An early and late role is also consistent with our previous pyrene rescue studies where we suggested that Leu191 pushed the uracil base in the early stages of the base-flipping process, and later served a plugging role to increase the lifetime of the base in the active site pocket (*7*). The pyrene rescue results reported in the following paper (*23*) further support an early and late role for Leu191.

Pulling by Asn123 and His187. Of these two putative pulling groups, only the removal of Asn123 shows a strong damaging effect on base flipping. Although we were not able to measure the binding kinetics with N123G, the weak binding and the absence of a tryptophan fluorescence change suggest that this Asn123 interacts late in the base-flipping process, although an additional early role cannot be excluded. The enormous 2-AP fluorescence increase upon N123G binding is so large it suggests that the removal of Asn123 may have carved out a hole in the base binding pocket that is large enough to allow partial or complete flipping of the 2-AP probe or, alternatively, that the DNA conformation is perturbed such that the 2-AP base becomes significantly more unstacked with its neighboring bases in the complex with N123G. The former explanation is intriguing because it implies that UDG could flip other bases, if the active site were sterically compatible. This is clearly possible because

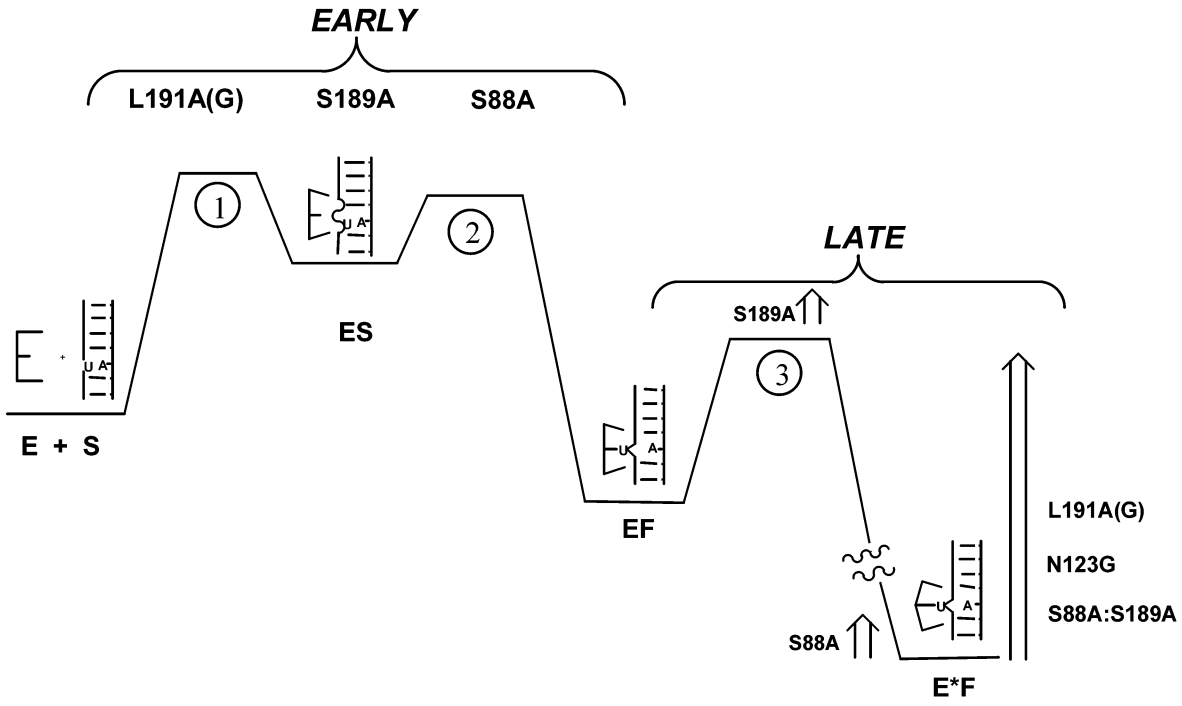

FIGURE 7: Free energy reaction coordinate diagram for the temporal action of the serine, leucine, and asparagine groups that are involved in the three-step pinch, push, plug, and pull base-flipping mechanism. The interactions are described loosely as "early" if they are important in the ground states or transition states that precede the formation of the EF intermediate and "late" if they are important in the formation or stabilization of the final docked complex (E*F). The first step involves formation of a weak nonspecific encounter complex (ES), which is rapidly isomerized in the second transition state to the extrahelical state detected by 2-AP fluorescence (EF). Removal of Leu191, Ser88, or Ser189 diminishes the rate of formation of the EF species. The E*F complex is severely destabilized (a late effect) when Leu191 or Asn123 is removed or when *both* Ser88 and Ser189 are removed (the long vertical arrow depicts this large destabilization). In addition, the S189A mutation destabilizes the transition state for formation of the E*F state, while the S88A mutation increases the energy of the ground state of the complex. These modest effects are depicted as short vertical arrows. To emphasize the energetic features of the pathway, the diagram is drawn on a roughly linear scale to correspond with the rate constants reported in Table 3.

UDG mutants that act on cytidine and thymidine nucleotides have been reported. However, there is no evidence that wtUDG can flip any other base into the active site pocket due to the strict steric constraints and optimized hydrogen-bonding groups that are specific for uracil (*2*, *10*).

The 5-fold smaller k_{on} for the H187G mutant may indicate an early or late role for this group, but removal of His187 has no large effect on the stability of the flipped-out base or that of the closed conformation. The observed effects of His187 on base flipping may arise from its interaction with uracil O2, and/or the short hydrogen bond between its backbone amide and the DNA phosphodiester backbone. These small effects on base flipping further highlight the primary role of His187 in transition-state stabilization (*29*).

Summary. The mutational studies performed here provide strong support for the stepwise nature of the base-flipping process by UDG that involves both an early destabilization of the DNA duplex, resulting in a metastable extrahelical state (EF, Figure 7), and a late conformational change in the enzyme that allows positioning of active site groups around the extrahelical base (E*F). This gating step is not detected with nonspecific DNA (*10*), and is abrogated by the removal of the Leu191 pushing and plugging group or the Asn123 pulling residue or when both of the hydroxyl side chains of the serine pinching groups are deleted (Figure 7). The uncoupling of the early and late steps in base flipping by mutagenesis has allowed assignment of the interactions of these side chains in the apparent transition states and ground states in both steps of the reaction. Remarkably, the substrate rescue studies that are described in the following paper show how the early and late effects can be fully rescued by a substrate that contains a pyrene nucleotide wedge (*23*).

SUPPORTING INFORMATION AVAILABLE

Kinetic simulations of the stopped-flow kinetic traces in Figure 4A,B,E,F and the associated Dynafit script files. This material is available free of charge via the Internet at http://pubs.acs.org.

REFERENCES

1. Klimasauskas, S., Kumar, S., Roberts, R. J., and Cheng, X. (1994) *Cell 76*, 357−69.
2. Parikh, S. S., Mol, C. D., Slupphaug, G., Bharati, S., Krokan, H. E., and Tainer, J. A. (1998) *EMBO. J. 17*, 5214−26.
3. Lau, A. Y., Wyatt, M. D., Glassner, B. J., Samson, L. D., and Ellenberger, T. (2000) *Proc. Natl. Acad. Sci. U.S.A. 97*, 13573−13578.
4. Barrett, T. E., Scharer, O. D., Savva, R., Brown, T., Jiricny, J., Verdine, G. L., and Pearl, L. H. (1999) *Embo J. 18*, 6599−609.
5. Bruner, S. D., Norman, D. P., and Verdine, G. L. (2000) *Nature 403*, 859−66.
6. Parikh, S. S., Walcher, G., Jones, G. D., Slupphaug, G., Krokan, H. E., Blackburn, G. M., and Tainer, J. A. (2000) *Proc. Natl. Acad. Sci. U.S.A. 97*, 5083−5088.
7. Jiang, Y. L., Kwon, K., and Stivers, J. T. (2001) *J. Biol. Chem. 276*, 42347−54.
8. Handa, P., Roy, S., and Varshney, U. (2001) *J. Biol. Chem. 276*, 17324−31.
9. Slupphaug, G., Mol, C. D., Kavli, B., Arvai, A. S., Krokan, H. E., and Tainer, J. A. (1996) *Nature 384*, 87−92.

10. Stivers, J. T., Pankiewicz, K. W., and Watanabe, K. A. (1999) *Biochemistry 38*, 952−63.
11. Stivers, J. T. (1998) *Nucleic Acids Res. 26*, 3837−44.
12. Dong, J., Drohat, A. C., Stivers, J. T., Pankiewicz, K. W., and Carey, P. R. (2000) *Biochemistry 39*, 13241.
13. Xiao, G., Tordova, M., Jagadeesh, J., Drohat, A. C., Stivers, J. T., and Gilliland, G. L. (1999) *Proteins 35*, 13−24.
14. Werner, R. M., Jiang, Y. L., Gordley, R. G., Jagadeesh, G. J., Ladner, J. E., Xiao, G., Tordova, M., Gilliland, G. L., and Stivers, J. T. (2000) *Biochemistry 39*, 12585−94.
15. Drohat, A. C., Jagadeesh, J., Ferguson, E., and Stivers, J. T. (1999) *Biochemistry 38*, 11866−75.
16. Drohat, A. C., Xiao, G., Tordova, M., Jagadeesh, J., Pankiewicz, K. W., Watanabe, K. A., Gilliland, G. L., and Stivers, J. T. (1999) *Biochemistry 38*, 11876−86.
17. Drohat, A. C., and Stivers, J. T. (2000) *Biochemistry 39*, 11865−75.
18. Drohat, A. C., and Stivers, J. T. (2000) *J. Am. Chem. Soc.* 1840−1841.
19. Wong, I., Lundquist, A. J., Bernards, A. S., and Mosbaugh, D. W. (2002) *J. Biol. Chem. 20*, 20.
20. Drohat, A. C., Jagadeesh, J., Ferguson, E., and Stivers, J. T. (1999) *Biochemistry 38*, 11866−11875.
21. Johnson, K. A. (1992) *Enzymes 20*, 1−61.
22. Kuzmic, P. (1996) *Anal. Biochem. 237*, 260−73.
23. Jiang, Y. L., Stivers, J. T., and Song, F. (2002) *Biochemistry 41*, 11248−11254.
24. Jiang, Y. L., Drohat, A. C., Ichikawa, Y., and Stivers, J. T. (2002) *J. Biol. Chem. 277*, 15385−15392.
25. Jiang, Y. L., and Stivers, J. T. (2001) *Biochemistry 40*, 7710−19.
26. Drohat, A. C., Xiao, G., Tordova, M., Jagadeesh, J., Pankiewicz, K. W., Watanabe, K. A., Gilliland, G. L., and Stivers, J. T. (1999) *Biochemistry 38*, 11876−11886.
27. Eftedal, I., Guddal, P. H., Slupphaug, G., Volden, G., and Krokan, H. E. (1993) *Nucleic Acids Res. 21*, 2095−101.
28. Bellamy, S. R., and Baldwin, G. S. (2001) *Nucleic Acids Res. 29*, 3857−63.
29. Stivers, J. T., and Drohat, A. C. (2001) *Arch. Biochem. Biophys. 396*, 1−9.

BI026226R